

Non-commutative theory of nonequilibrium reveals Cantor triadic set in a rich ensemble of coalescing distributions

Jérôme CHAUVET*

ABSTRACT

Mathematics of non-commutative spaces is a rapidly growing research field, which has to date found convincing proof of its legitimacy in the nature, precisely, in quantum systems. In this paper, I evaluate the extension of fundamental non-commutativity to the theory of chemical equilibrium in reactions, of which little is known about its phenomenological implication. To do so, I assume time to be fundamentally discrete, with time values taken at integer multiples of a time quantum, or chronon. By integrating chemical ordinary differential equations (ODE) over the latter, two non-commutative maps are derived. The first map allows excluding some hypothetical link between chemical Poisson process and uncertainty due to non-commutativity, while the second map shows that, in first-order reversible schemes, orbits generate a rich collection of non-equilibrium statistics, some of which have their support close to the Cantor triadic set, a feature never reported for the Poisson process alone. This study points out the need for upgrading the current chemical reaction theory with non-commutativity-dependent properties.

* Contact: jerome.chauvet.msc@gmail.com

INTRODUCTION

Not only quantity and velocity are crucial characteristics in describing a particular process. If we let us envisage a naive scientist, one so eager that he would start writing his research report *before* possessing results to deal with in it, then we seize at once how out of inspiration his brain is going to run, and how *after* this scientist ought to have written it, in any sensible manner. This is, in fact, a general requirement to all complex processes. Recipe cooking, chess strategy, room tidying, and so on, there exists in the everyday life tons of complex processes, i.e., processes being a combination of singular well-defined sub-processes, which consist in a particular ordering of elementary parts, but for which another order of them would not let the resulting action fulfil the wished purpose. This particular property for two elementary transformations to be not trivially exchangeable is referred to as non-commutativity¹.

And not only macroscopic evidences can be given. At the microscopic level, the inner and irreducible non-commutativity in the description of matter by quantum theory renders this fact inevitable in the debate². However, although macroscopic systems, if smart, can by themselves compute and find what proper order to set up in view of a particular goal, very simple microscopic ones remain unable to perform any reasonable choice of an order or another, for they are not expected to have sorting ability. Historically, it was M. Born and P. Jordan who first built an explicit algebraic bridge between the probabilistic nature of microscopic systems and the non-commutativity in their theoretical description by matrix operators, proving thereby that real systems should inherit phenomenological properties from their formal form^{3,4}.

In spite of its universality, rarely is non-commutativity specifically studied in natural systems other than quantum ones. This is true even when that theory is mathematically based on matrix algebra, and even if the so-called theory deals with uncertainty in the process. Beside this, one important field, in which non-commutativity arises, is analysis of partial differential equations (PDE). In deed, when resolving the latter, or attempting to do so, it is of use to split operators into two or more of them in order to facilitate solution determination of the corresponding dynamical systems⁵. One then analyzes the added bias due to the frequent non-commutativity born from operator duplication. However, lack of commutativity is, in this particular case, considered to be generating non relevant errors, and not promoting novel property discovery⁶.

In chemical reaction networking, in which high dimensionality meets the matrix requirement, and in which structural complexity is some constant source of uncertainty⁷, one can deplore such a gap of knowledge. But to date, neither the deterministic description based on ODE systems, nor the probabilistic theorization provided by the chemical master equation, were at the origin of investigations chasing specific effects causally related to non-commutativity. Such an investigation appears though now to be pressing, as many recent advances, which involve information management by large chemical systems, especially biochemical networks, raise the question of the reliability of this information in noisy environment⁸⁻¹². Thus, this article aims at identifying non-commutativity in the most simple reaction systems, and estimating its phenomenological consequences on clear physical basis, in view of future development.

This paper is organized as follows. First part deals with the general approach and notations used over the whole report. In the second part, I confront the well-established Poissonian chemical uncertainty and a conception of uncertainty due to non-commutativity. Finally, third part aims at numerically analyzing the non-equilibrium dynamics specifically due to non-commutativity in the reversible scheme.

1. GLOBAL APPROACH, NOTATIONS

I based this work on transformations of ODE smooth solutions into recursive maps over a time dimension that is discontinuous in the most fundamental manner. Time discretization will be assumed to be fundamental through consideration of a minimal generator for time values, i.e., a chronon, which will be denoted θ . The latter should be interpreted as the minimal time duration, during which no modification of the system state is possible, as no transfer of mass or of information from external source may intervene within that time. In this view, θ is akin to Caldirola's chronon^{13,14} and Planck's time, at the shortest physical limits. However, determining its precise value in the case of an arbitrary chemical system is, at that time, still a challenging issue, so we will treat θ as an open value in this paper. In doing so, reaction events become discontinuous, no matter how high the considered concentrations of reactants and products are.

Recursive maps will be derived from ODE smooth solutions through the following procedure. Let $\varpi(t)$ be some unknown function of time t , K some constant, Φ the indefinite integral of

function ϕ , and Φ^{-1} the inverse function of Φ . Then, out of any separable linear first-order ODE derived from the law of mass action, for which:

$$\int_{\varpi(t)}^{\varpi(t+\theta)} \phi(\varpi(t)) d\varpi(t) = \int_t^{t+\theta} K dt \quad (1.0)$$

holds, one obtains a map straightforwardly in the form:

$$\varpi(t + \theta) = \Phi^{-1}(K\theta + \Phi(\varpi(t))) \quad (1.1)$$

Throughout this article, ϖ_t will stand for a global state vector comprising all chemical entities concentration of the reaction at time $t = n\theta$, with n being positive integer. The special case of initial condition will be denoted $t = 0 \times \theta := i$. Also, constant:

$$\kappa_a = e^{-k_a \theta} \quad (1.2)$$

where subscript a refers to some particular half-reaction, will recurrently be used for better readability of formulas.

2. NON-COMMUTATIVE INTERPRETATION OF THE POISSON PROCESS

Uncertainty in reaction processes is broadly assumed to be Poissonian¹⁵, which is analytically proved true for some simple chemical networks by means of the master equation approach¹⁶. I test here whether or not Poissonian behaviour should be related to some fundamental non-commutativity, in some typical reaction scheme. The latter will be the mono-molecular pure death process of a reactant r into a product p . Its recurrent mapping, elaborated with method (1.0), is easily shown, for n being the n^{th} iteration of the map, to be:

$$\varpi_{t+n\theta} = \begin{bmatrix} r_{t+n\theta} \\ p_{t+n\theta} \end{bmatrix} = \begin{bmatrix} \kappa^n & 0 \\ (1 - \kappa^n) & 1 \end{bmatrix} \varpi_t \quad (2.1)$$

When put into semantic form, the operator of (2.1) means the following:

“Draw from r a quantity that is proportional to κ while transferring it directly into p ”.

Bearing in mind that Poissonian noise occurs where concentration is transferred from reactant to product, let us try and build a non-commutative interpretation of this statement by breaking up the previous assertion into a couple of the same but now segmented semantic value, which yields:

- a – “Pick a quantity from r that is proportional to κ “
- b – “Put this quantity into p “

Then, let us assign a different operator to each of these assertions. Each operator will stand for either the semantic value of a, as an operator noted R , or the semantic value of b, as an operator noted P . This yields the following couple:

$$R = \begin{bmatrix} \kappa & 0 \\ 0 & 1 \end{bmatrix} \quad P = \begin{bmatrix} 1 & 0 \\ (1-\kappa) & 1 \end{bmatrix} \quad (2.2)$$

Given this couple of operators, the only way to recover a map that would be some equivalence to (2.1) is to compose R and P in a matrix product. This is a multiplicative split of the operator in (2.1). In this case, it is of common use to calculate the commutator of this product, which here is found to be:

$$[R, P] = RP - PR = \begin{bmatrix} 0 & 0 \\ (1-\kappa)^2 & 0 \end{bmatrix} \quad (2.3)$$

This commutator varies according to κ , which itself depends on both kinetics constant k and chronon θ , the two of which are positive real numbers. Thus, relation (2.3) demonstrates the non-commutativity of matrix multiplication between R and P . Note that this commutator never equals to the null-matrix, except when considered in the limit of continuity, that is to say:

$$\lim_{\theta \rightarrow 0} [R, P] = 0 \quad (2.4)$$

Hence, the RP product becomes commutative only for θ tends to infinitesimal chronon duration dt , otherwise not.

Now, let us construct a new recursive map by means of the two operators of (2.2). Let us also invoke, here, a third novel operator, so as to obtain the following map:

$$\varpi_{t+n\theta} \equiv C^n(R, P)\varpi_t \quad (2.5)$$

This C will be called a choice operator, defined as the operator taking two arbitrary square matrices of the same order in its arguments field, and multiplying them with either one order or the other. When put to its n^{th} power, like in (2.5), C performs its action n times on initial values in a multiplicative chain of the following form:

$$C^n(R, P) \sim \prod_{u=1}^{2^n} (b_u RP + (1-b_u)PR) \quad (2.6)$$

In (2.6), the only constraint put on b_u is that it is every u^{th} element of any arbitrary sequence of 1's and 0's taken from $\{0,1\}^{2^n}$, together with the convention $C^0(R, P) = \text{Diag}(1,1,\dots,1)$. Due to the non nullity of (2.3) when time is discrete, it comes that the map orbit then generated is in the form of a rooted tree¹⁷. From (2.6) should be deduced any walk throughout the vertices space of the associated tree, from root, i.e. $C^0(R, P)\varpi_i$, to boundary, i.e. $C^\infty(R, P)\varpi_i$. At each step of the recursive process, non-commutativity of the RP product engenders state duplication, and we are logically led to relate (2.1) to (2.5).

To do so, it is necessary to demonstrate the possibility for the tree of (2.5) to be parameterized, so as to access every nodes of it by means of one single value. Thus, let:

$$\varpi_{n+1} \equiv \begin{cases} RP\varpi_n = \begin{bmatrix} \kappa r_n \\ (1-\kappa)r_n + p_n \end{bmatrix} \\ PR\varpi_n = \begin{bmatrix} \kappa r_n \\ \kappa(1-\kappa)r_n + p_n \end{bmatrix} \end{cases} \quad (2.7)$$

ϖ has an upper coordinate r , which is invariant under multiplication order inversion, so we can parameterize its time-dependent evolution by means of one single integer value n , and initial condition r_i . This is easily found to be the following:

$$r_n = \kappa^n r_i \quad (2.8)$$

Unlike (2.8), the lower coordinate of ϖ , i.e. p , is affected by non-commutativity, and we have state duplication at this particular coordinate:

$$p_{n+1} \equiv \begin{cases} (1-\kappa)r_n + p_n \\ \kappa(1-\kappa)r_n + p_n \end{cases} \quad (2.9)$$

Relation (2.9) demonstrates that the map orbit is in the form of a tree at coordinate p , but not at coordinate r . Thanks to (2.8), we are prompted to re-write (2.9) and make it so that r is no more dependent on time parameter n . Thus:

$$p_{n+1} \equiv \begin{cases} \kappa^{n+[0]}(1-\kappa)r_i + p_n \\ \kappa^{n+[1]}(1-\kappa)r_i + p_n \end{cases} \quad (2.10)$$

Notice that the square brackets are here conventional ones, enrolled for the purpose of pointing out the special value put in between them, i.e. 0 or 1. That pair of values provides, at each single step of the process, a binary signature of the choice for one order of multiplication or the other, that is to say, the b_u values of (2.6).

As to express p_n in the form of a function of initial condition p_i and positive integer n , let us consider such a state duplication recursively, until step time 0 has been reached. It yields:

$$\begin{aligned}
p_{n+2} &\equiv \begin{cases} \kappa^{n+1+[0]}(1-\kappa)r_i + p_{n+1} \\ \kappa^{n+1+[1]}(1-\kappa)r_i + p_{n+1} \end{cases} \\
&\equiv \begin{cases} \begin{cases} \kappa^{n+1+[0]}(1-\kappa)r_i + \kappa^{n+[0]}(1-\kappa)r_i + p_n \\ \kappa^{n+1+[0]}(1-\kappa)r_i + \kappa^{n+[1]}(1-\kappa)r_i + p_n \end{cases} \\ \begin{cases} \kappa^{n+1+[1]}(1-\kappa)r_i + \kappa^{n+[0]}(1-\kappa)r_i + p_n \\ \kappa^{n+1+[1]}(1-\kappa)r_i + \kappa^{n+[1]}(1-\kappa)r_i + p_n \end{cases} \end{cases} \quad (2.11)
\end{aligned}$$

Considering (2.11) recursively up to any m^{th} step finally leads to:

$$p_m \equiv (\kappa^{m-1+b_1} + \kappa^{m-2+b_2} + \dots + \kappa^{m-m+b_m})(1-\kappa)r_i + p_i \quad (2.12)$$

In (2.12), each b_j equals to either 0 or 1, so a whole infinite sequence of them encodes one particular orbit from root to boundary of the tree. One is prompted to reduce the writing of (2.12) by changing the parameterization system, as demonstrated hereafter.

Let $b_1b_2\dots b_n$ be some binary code of length n such that each $b_j \in \{1,0\}$. Let the following parameterization system:

$$\bar{\omega}_n \sim \bar{\omega}_{b_1b_2\dots b_n} = \begin{bmatrix} r_n \\ P_{b_1b_2\dots b_n} \end{bmatrix} \quad (2.13)$$

Then, one can quietly claim that:

$$\bar{\omega}_{b_1b_2\dots b_n} \equiv C^n(R, P)\bar{\omega}_i \quad (2.14)$$

Moreover, an explicit form for the choice operator is found to be:

$$C^n(R, P) := \begin{bmatrix} \kappa^n & 0 \\ (1-\kappa)\sum_{j=1}^n \kappa^{n-j+b_j} & 1 \end{bmatrix} \quad (2.15)$$

In (2.14), the binary code $b_1b_2\dots b_n$ encodes time information by means of its index, i.e. 1 to n , while values themselves, i.e. 0 and 1, encode the choice for one order of multiplication or the other, defined for each j^{th} step of the map. Expression (2.10) demonstrates that 0 encodes multiplication order for RP , and 1 for PR . Hence, the binary parameterization of the tree has been demonstrated.

To validate the hypothesis that the non-commutative model is a correct theory for the pure death process reaction, it is essential to resort to some fundamental principle. The motivation for this is that the tree consists in a time-dependent exponential expansion of possible states at the product side of the reaction but not at the reactant side of it, so one is prompted to investigate which ones of these states are consistent with the principle regulating the overall mass of the system. Naturally, mass conservation will be this particular principle, through the use of a mass hyper-surface. As a matter of fact, we need to prove true, for all n and for all $b_1b_2\dots b_n$, the following relation:

$$r_n + p_{b_1b_2\dots b_n} - (r_i + p_i) = 0 \quad (2.16)$$

Combining (2.15) and (2.16), the above relation becomes:

$$\begin{aligned} \kappa^n r_i + (1 - \kappa) \sum_{j=1}^n \kappa^{n-j+b_j} r_i + p_i &= r_i + p_i \\ \Leftrightarrow \kappa^n + (1 - \kappa) \sum_{j=1}^n \kappa^{n-j+b_j} &= 1 \end{aligned} \quad (2.17)$$

Let now the sub-set of particular finite walks of length n encoded by all finite sequences such that every $b_j = 0$, where $0 \leq j \leq n$. This corresponds to any walk for which the product entity appears after reactant entity has reacted. Hence (2.17) becomes:

$$\kappa^n + \kappa^n (1 - \kappa) \sum_{j=1}^n \kappa^{-j} = 1 \quad (2.18)$$

Then, using the well-known formula for the sum of all terms of a geometric sequence up to n , we obtain:

$$\begin{aligned} \kappa^n + \kappa^n(1-\kappa) \left[\frac{1-\kappa^{-(n+1)}}{1-\kappa^{-1}} - 1 \right] &= 1 \\ \Leftrightarrow (\kappa^{-1}-1)\kappa^n &= (\kappa^{-1}-1)\kappa^n \end{aligned} \quad (2.19)$$

(2.19) is true for all n , thus demonstrating that the particular map orbit determined by all state vectors of the form $\overline{\omega}_{00\dots 0}$ preserves mass conservation all along the walk. Any other kind of walk will have one or more 1's in its binary parameter, so that we will have to substitute one 0 for one 1 at each d^{th} digit of a given set Δ of non-redundant indices in the coding sequence. Given (2.18), we deduce that this yields:

$$\begin{aligned} \kappa^n + (1-\kappa) \left(\sum_{j=1}^n \kappa^{n-j+0} - \sum_{d \in \Delta} \kappa^{n-d+0} + \sum_{d \in \Delta} \kappa^{n-d+1} \right) &= 1 \\ \Leftrightarrow \kappa^n + \kappa^n(1-\kappa) \left(\sum_{j=1}^n \kappa^{-j} - \sum_{d \in \Delta} (\kappa^{-d}(1-\kappa)) \right) &= 1 \end{aligned} \quad (2.20)$$

Considering triviality of equation (2.18), (2.20) turns out to be:

$$-\kappa^n(1-\kappa)^2 \sum_{d \in \Delta} \kappa^{-d} = 0 \quad (2.21)$$

If Δ is finite, then (2.21) holds if κ equals to 1, i.e., in the continuous limit situation $\theta \sim dt$, which pulls this case out of the discontinuity statement; otherwise, (2.21) holds for $n \sim +\infty$, i.e., at an effective infinite time, which is neither observable nor calculable. If Δ is infinite, then n must tend to infinity too, as $\Delta \subseteq n$, which is to be rejected with the same argument as in the previous case. In the end, we conclude that:

- Since the multiplication order encoded by 0 refers to product order RP , and not product order PR , the above inspection justifies the trivial order again, i.e., the order such that reactant must disappear first before product can appear, which is commonly assumed in schematic form by the arrow direction of $r \xrightarrow{k} p$.
- Since orbits of the form $\overline{\omega}_{00\dots 0}$ are the only acceptable ones, the underlying Poisson process, with respect to the idea that it is uncertainty in the transformation from reactant to product, should not be imputed to non-commutativity.

3. COMPETING REACTIONS AND UNCERTAINTY

Irreversible first-order reactions are rare as compared to reversible ones. Most of the time, the backward reaction exists, and one ought not to neglect it unless its rate is drastically slow. Due to this, an ambiguous situation, in which both $x \xrightarrow{k_+} y$ and $y \xrightarrow{k_-} x$ are valid at the same time, arises. Hence, competing half-reactions generates outcome indetermination, which hereafter I analyze from the non-commutative point of view.

Let us adapt the theory to the reversible case. The state vector will now be $\varpi = (x, y)$, and elementary events will be semantically defined so:

a – “Draw from x a quantity that is proportional to κ_+ while transferring it directly to y ”

b – “Draw from y a quantity that is proportional to κ_- while transferring it directly to x ”

Again here, we associate one operator acting on the state space with each statement above, each of which should correspond to either the forward half-reaction (+ subscript), i.e. assertion “a”, or the backward half-reaction (– subscript), i.e. assertion “b”. One thus has:

$$Q_+ = R_+ P_+ = \begin{bmatrix} \kappa_+ & 0 \\ (1-\kappa_+) & 1 \end{bmatrix} \quad Q_- = R_- P_- = \begin{bmatrix} 1 & (1-\kappa_-) \\ 0 & \kappa_- \end{bmatrix} \quad (3.1)$$

At each step of the process, a complete reaction event necessarily consists in the action of both operators, so we have to multiply Q_+ and Q_- . The associated commutator equals to:

$$[Q_+, Q_-] = (1-\kappa_+)(1-\kappa_-) \begin{bmatrix} -1 & -1 \\ 1 & 1 \end{bmatrix} \quad (3.2)$$

With the same arguments as those invoked for (2.3), this commutator is no null-matrix except in the limit of time continuity (i.e. $\theta \sim dt$), and proves non-commutativity to be a non negligible feature of the reversible system. I recall here that time discretization meets a fundamental justification because there exists, in any two coupled chemical reactions, a duration equalling to at least Planck’s time, within which neither chemical process is able to either be disturbed by or disturb the other one, so each half-reaction must be an isolated system in a period spanning over one chronon.

One immediately validates the model using the mass conservation relation.

It is, in fact, straightforward to assert that composing this couple of operators conserves mass. In deed, each single operator Q_+ and Q_- individually conserves mass, as already demonstrated in Section 2 (cf. 2.19), so that applying one operator then the other to the state vector does map mass with respect to that conservation, whatsoever the composition order is. Hence, one will simply assume the following to hold for any value of the binary parameter:

$$x_{b_1 b_2 \dots b_n} + y_{b_1 b_2 \dots b_n} - (x_i + y_i) = 0 \quad (3.3)$$

As per Section 2, one is led to state that the map for the reversible first-order scheme has the following form:

$$\begin{aligned} \varpi_{b_1 b_2 \dots b_{p+q}} &\equiv C^p(Q_+, Q_-)\varpi_{b_1 b_2 \dots b_q} \\ &\equiv C^{p+q}(Q_+, Q_-)\varpi_i \end{aligned} \quad (3.4)$$

In (3.4), C^n is the n^{th} iteration of the choice operator previously defined in Section 2. The consequence of applying C recursively to the state vector will be captured by calculation of the non-commutativity-dependent divergence δ , that is to say, the following relation:

$$\begin{aligned} \delta \varpi_{b_1 b_2 \dots b_n b_{n+1}} &= Q_+ Q_- \varpi_{b_1 b_2 \dots b_n} - Q_- Q_+ \varpi_{b_1 b_2 \dots b_n} \\ &= [Q_+, Q_-] \varpi_{b_1 b_2 \dots b_n} \end{aligned} \quad (3.5)$$

Combined with (3.3), (3.5) is found to be:

$$\delta \varpi_{b_1 b_2 \dots b_{n+1}} = (1 - \kappa_+)(1 - \kappa_-)(x_i + y_i) \begin{bmatrix} -1 \\ 1 \end{bmatrix} \quad (3.6)$$

From (3.6) must be deduced that the divergence caused by non-commutativity affects both coordinates of the state vector and, moreover, that it is stationary since (3.6) does not depend on n . Therefore, the orbit triggered by the map (3.4) is in the form of two rooted trees, one per dimension of the system, with root at time 0 and exponential expansion of base 2 at boundary.

Furthermore, because of the unconditional validity of (3.3), all possible walks through them are consistent with the mass conservation principle.

At this point, an explicit binary parameterization of (3.4) would be essential for a deep comprehension of this map. However, in this pioneering work, I was not able to exhibit such a parameterized form, so I was led to opt for an estimation of the tree structure using a probabilistic method, namely the Monte-Carlo method. Since (3.4) models the step-by-step undetermined outcome of two competing half-reactions due to the constitutive randomness of events occurring at the molecular level, this map was numerically simulated as if it were some stochastic process of which no exact solution is known. In deed, (3.4) deploys, at each recursion step, a set of co-temporal states and not a single path and, in such a case, it is judicious, if no formal solution is available, to randomly render one plausible trajectory among all possible ones, and assume this being a representative realisation of the general solution¹⁸. Implementation of Monte-Carlo estimation of the tree is detailed in appendix A. A large amount of values for kinetics constants and initial conditions was probed, which have always led to the same type of results. One typical distribution series, obtained with $k_+ = 0.3234$ and $k_- = 0.2822$, is shown in Fig.1.

In Fig. 1, augmenting θ as continuously as can be (i.e., in the numerical sense of it) from 0 to positive infinity has the effect to let the system dynamics generate different distributions, every of which smoothly deform from one into another as a direct function of chronon duration θ . I found some of those distributions to be of special interest, which from now on will be mentioned as key-distributions, and detailed hereafter.

For $\theta \rightarrow 0$, i.e. $\theta \sim dt$, statistics around the equilibrium is in the form of a Dirac distribution, i.e., tending to the analytic flat solution. At $\theta = 0.3729$, the system has shifted from the Dirac distribution to some bell-shaped distribution, which resembles a Gaussian distribution. The latter was confirmed by numerical computing of the fit to the Gaussian normal distribution curve, which gave the correlation coefficient $R^2 = 0.9967$ with this particular set of constants. Around $\theta = 0.8559$, the relative frequency distribution is in the form of a Takagi triadic function¹⁹. Around $\theta = 1.147$, states distribution has come down back to a more common statistics density, which is the uniform one. In fact, the latter seems to be the very upper limit of a distribution sub-set related to the interval defined by $\theta \in [0, 1.147]$, and of shared characteristic that their support appears to be connected. In deed, as soon as $\theta > 1.147$

(for instance $\theta = 1.21$ here) uniform distribution breaks up into a set of sub-distributions, which jointly produce a global statistics with disconnected support. Moreover, those disconnected supports resemble a known class of geometrical set, namely the Cantor set²⁰. To add visual evidences to this conjecture, I checked if the Cantor triadic set C_3 , which I calculated in Fig.1.(g) up to the third iteration of its construction rule, matches one or more sub-supports, for some value of chronon θ , and found, at $\theta = 1.76201$, such a match to be convincing, provided the triadic Cantor set, which is currently constructed out of the unity segment, was linearly stretched so as to fit the overall support. Finally, as θ tends to be infinitely long, global distribution progressively fuses into a pair of peaks, one at 0, and the other at $x_i + y_i$. This limit statistical behaviour is already clear in Fig.1.(h) as soon as $\theta = 10.3989$, and rigorous proof of this limit distribution is developed hereafter.

Let the two limit operators A and B, such that:

$$A = \lim_{\theta \rightarrow +\infty} Q_+ = \begin{bmatrix} 0 & 0 \\ 1 & 1 \end{bmatrix} \quad B = \lim_{\theta \rightarrow +\infty} Q_- = \begin{bmatrix} 1 & 1 \\ 0 & 0 \end{bmatrix} \quad (3.7)$$

The individual first action of either operator of (3.7) on ϖ_i , in the limit of θ tends to infinity, is either:

$$A \begin{bmatrix} x_i \\ y_i \end{bmatrix} = \begin{bmatrix} 0 \\ x_i + y_i \end{bmatrix} \quad (3.8)$$

Or:

$$B \begin{bmatrix} x_i \\ y_i \end{bmatrix} = \begin{bmatrix} x_i + y_i \\ 0 \end{bmatrix} \quad (3.9)$$

Let $M = x_i + y_i$. Then, any subsequent mapped value is in one of the four following cases:

$$A \begin{bmatrix} 0 \\ M \end{bmatrix} = \begin{bmatrix} 0 \\ M \end{bmatrix} \quad A \begin{bmatrix} M \\ 0 \end{bmatrix} = \begin{bmatrix} 0 \\ M \end{bmatrix} \quad B \begin{bmatrix} M \\ 0 \end{bmatrix} = \begin{bmatrix} M \\ 0 \end{bmatrix} \quad B \begin{bmatrix} 0 \\ M \end{bmatrix} = \begin{bmatrix} M \\ 0 \end{bmatrix} \quad (3.10)$$

Moreover, the algebra made of the two operators A and B has a non-Abelian group structure demonstrated by the four following equalities:

$$\begin{aligned}
A^2 &= A \\
B^2 &= B \\
AB &= A \\
BA &= B
\end{aligned}
\tag{3.11}$$

Hence, it has been demonstrated that any n^{th} action of the choice operator on the state space, in the limit of θ tends to infinity, yields either vector $(0, M)$, or vector $(M, 0)$. Furthermore, since both operators act with probability $1/2$ in the Monte-Carlo estimation of the tree, statistics happens in turn to be strictly bimodal, with one peak at 0 , and the other one at M , of respective relative frequency $1/2$.

For a given real system, if θ has been fixed, one can directly calculate the real kinetics constants, which match the simulated statistics using the invariance relation below:

$$k_{\rho}\theta_{\rho} = k_{\nu}\theta_{\nu} \tag{3.12}$$

In (3.12), k refers to kinetics constant, θ refers to chronon, subscript ρ refers to the real system, and subscript ν refers to the numerical system used as data source. Invariance relation (3.12) allows exploring values for parameters while keeping (1.2), and hence the corresponding statistics, unchanged. Some examples of conversion, performed with reference values Planck's time and Caldirola's chronon, together with the previous numerical data presented in Fig.1, are shown in Fig.2.

Fig.2 shows that, in a range spanning over all special distributions of the theory, real kinetics constants roughly have the order of magnitude of one hundredth of the real chronon reciprocal. Interestingly, it can be stated a necessary and sufficient emergence condition on the appropriate magnitude for kinetics parameters, which prompts a real system to behave according those key-distributions. In deed, since here $k_{+} \approx k_{-}$, one may reduce this information by assuming that k_{ν} approximately equals to $(k_{+} + k_{-})/2 = (0.3234 + 0.2822)/2 \approx 0.3$. Beside this, finding a satisfying interval for the corresponding k_{ρ} , which would span over all the so-called key-distributions, is formally

translated into $k_{\rho \min} \leq k_{\rho} \leq k_{\rho \max}$. Using (3.12), the latter transforms into $(\theta_{v \min} / \theta_{\rho})k_v \leq k_{\rho} \leq (\theta_{v \max} / \theta_{\rho})k_v$, then into $\theta_{v \min}k_v \leq \theta_{\rho}k_{\rho} \leq \theta_{v \max}k_v$. From numerical data (cf. Fig.1 and Fig.2), both boundaries are calculated to be at least $\theta_{v \min}k_v = 0.022 \times 0.3 = 7/1000$, and at most $\theta_{v \max}k_v = 10.4 \times 0.3 = 3.12 \approx 7/2$, the latter being majored so as to allow arithmetic reduction, and altogether this yields the remarkable condition:

$$\frac{1}{1000} \leq \frac{1}{7} \theta k \leq \frac{1}{2} \quad (3.13)$$

In (3.13), subscripts have been removed since, according to (3.12), (3.13) applies to both numerical and real systems. Inequalities (3.13) hold for any first-order reversible reaction having both forward and backward kinetics constants close in value to each other.

Like kinetics constants and chronon do, initial conditions also transform statistics into other ones when they are varied. Hence, we need to determine what class of transformation is concerned in that variation so as to evaluate the significance of initial conditions in the qualitative description of these statistics. To infer this, one may resort to the choice operator linearity, as done hereafter.

Let three arbitrary initial state vectors (x_i, y_i) , (x'_i, y'_i) and (x''_i, y''_i) . Let C^n be the n^{th} iteration of the choice operator, and C^n_{ij} be its coefficient at the i^{th} row and j^{th} column. Let p_u, p'_u, p''_u and P_u, P'_u, P''_u denote respectively the lower and the upper edge of a given partition region on dimension u associated with the three initial vectors above. By linearity, one is allowed to write:

$$C^n \begin{bmatrix} x_i + x'_i \\ y_i + y'_i \end{bmatrix} = C^n \begin{bmatrix} x_i \\ y_i \end{bmatrix} + C^n \begin{bmatrix} x'_i \\ y'_i \end{bmatrix} \quad (3.14)$$

Every statistics generated through iteration of the choice operator are counts per region of the state space partition, which the map orbit has visited, e.g. when the system is in $[p_u, P_u]$. Because of this last point and since (3.14) holds, one is impelled to write that if:

$$\begin{cases} p_x \leq C_{11}^n x_i + C_{12}^n y_i \leq P_x \\ p_y \leq C_{21}^n x_i + C_{22}^n y_i \leq P_y \end{cases} \quad (3.15)$$

is true (resp. false) for some n , and if:

$$\begin{cases} p'_x \leq C_{11}^n x'_i + C_{12}^n y'_i \leq P'_x \\ p'_y \leq C_{21}^n x'_i + C_{22}^n y'_i \leq P'_y \end{cases} \quad (3.16)$$

is also true (resp. false) for the same n , then:

$$\begin{cases} p_x + p'_x \leq C_{11}^n (x_i + x'_i) + C_{12}^n (y_i + y'_i) \leq P_x + P'_x \\ p_y + p'_y \leq C_{21}^n (x_i + x'_i) + C_{22}^n (y_i + y'_i) \leq P_y + P'_y \end{cases} \quad (3.17)$$

i.e.:

$$\begin{cases} p''_x \leq C_{11}^n (x''_i) + C_{12}^n (y''_i) \leq P''_x \\ p''_y \leq C_{21}^n (x''_i) + C_{22}^n (y''_i) \leq P''_y \end{cases} \quad (3.18)$$

is, in the end, also true (resp. false) for that n . The appropriate conclusion to this is that varying initial conditions without changing kinetics constants and chronon has no other effect than performing a linear lateral stretch of distributions, but with global shape that remains qualitatively unchanged. Therefore, kinetics constants and chronon duration are necessary and sufficient control parameters to have the system pass through the set of key-distributions described here, within the approximated range provided by (3.13)

DISCUSSION

The theory presented here is valid in the limit of high concentrations, since it ousts *de facto* the variability due to underlying Poisson processes, known to vanish at such a limit. It has been shown that non-commutativity does not cause Poissonian uncertainty, but that it generates besides, in the reversible case, its own non-equilibrium statistics. The theory strictly depends on the existence of a time quantum, also named chronon, a theoretical statement that

has not been yet experimentally clarified, but which, here, has found a plausible pathway to its proof of existence.

In PDE solution estimation methodology, splitting of operators consists in some cases in the artificial decoupling of naturally coupled phenomenon, with the intention of approximating solution of the coupled system; the disadvantage of this is the concomitant and inevitable emergence of inconsistency⁶. However, as shown in this report, operator splitting may no longer be interpreted as an approximation method if this coupling disruption meets a fundamental justification. In this idea, θ appears to be the key value of the theory. As primary instances of θ , Planck's time – i.e. the photon quantum of time – was taken as the lowest imaginable universal value for θ , and Caldirola's chronon – i.e. the electron quantum of time – was taken as the all first and historical attempt of time discretization for a particle endowed with mass and charge. However, a generalization of θ to all chemical compounds is still to be discovered, which would make the theory quantitatively robust in its predictions. As Caldirola's theory suggests it^{13,14}, such a generalized θ should be highly dependent on mass and charge of the molecular system under consideration. More precisely speaking, θ may in particular grow up concomitantly with mass, as revealed in the compared use of Planck's time and Caldirola's chronon for the computation of real kinetics constants. The question of the charge, which is a complex feature in large molecules, leaves however this point much too intricate for an ascertained conclusion here. In any case, future developments should always consider time to be the typical value in the causal order formally provided by maps, and should not take into account divergences in the time ranging less than one chronon, notably through τ -entropy determination, as it is assumed to be the case in chemical master equation approaches¹⁶.

Observation, in real reaction systems, of distributions having Cantorian support are expected to occur in first-order reversible schemes having two half-reactions with very high rates each, to push the system into the frame of the emergence condition inequalities. Note that M. Wilkinson came across spectacular Cantor sets studying formally electrons in incommensurable systems²¹, but it is more relevant to make, here, the connection with the coalescence observed in nuclear magnetic resonance (NMR) spectrometry, a technique with which one analysis, in isomers, the rapid internal reaction of passing from one stable configuration to the other²². Such reactions are, in standard conditions, usually modelled using law of mass action relations, but as NMR plunges those systems in electro-magnetic fields, one rather models them using Bloch's equation²³. It is known that isomerization reactions

have rates that are rather high, e.g. in the order of $4.0 \times 10^{10} \text{ s}^{-1}$ for the pent-1-en-4-yne²⁴, and that their dynamics takes place at the picosecond time-scale, e.g., in the rhodopsin isomerization from 11-cis to all-trans²⁵, which puts such systems in suitable condition for attaining specific effects of the theory. What has been shown here is a multi-branched fork of several levels of concentration, i.e. multimodality, a property that emerges here for the first time in linear reaction schemes. The coalescence detected in NMR experiments also generates forks, which however have a functional relation with temperature for modulating coalescence, and not kinetics constants or chronon duration like in this study. Coalescence in NMR experiments takes place in the resonance frequency domain, and not in the concentration domain, so all comparisons on this point should be discussed with care. Strong analogies and connections are, however, obvious to the eyes. Both coalescences occur in the same exchange reaction scheme, and emergence of forks should be, in the future, envisaged for that scheme with or without NMR environment. Also, kinetics parameters and temperature can be put in functional relation through the use of the Eyring equation or of the Arrhenius law²⁶, which renders both coalescences functionally tied to each other at the level of their control parameters. Also, signal in the form of a Cantor set resembles the peak repartition along the frequency scale of some ABX spin systems obtained in NMR spectroscopy, e.g. the 60-Mc fluorine resonances of 2-fluoro-4,6-dibromophénol²⁷. All in all, this novel role of non-commutativity in high-rated first-order reversible reactions might explain why isomerization reactions, which are fast-rated reactions, are poorly predicted by common statistical models, while the latter prove to be satisfying for slow-rated reactions^{28,29}. As an exciting and concrete consequence of this, the theory appears as a promising component in comprehending the recently characterized intrinsically unfolded proteins (IUP). In deed, that class of biomolecules is thought, in biological networks, to be endowed with large spectra of partners because of an ability to have many stable conformations, and to rapidly transform from one into another so to adapt to all of them^{30,31,32}. The importance of concentration levels in binding kinetics implies the importance of a fine model describing those levels, and this new theory might have a crucial role to play in that description. Naturally, further investigations will be needed to establish, in the most irrefutable way, all of these assertions.

In this logic, identification of distributions with their support belonging to the class of Cantor set – in particular the triadic Cantor set C_3 – is strategic, because it provides the theory with a straightforward bridge towards novel mathematical tools developed in the field of non-commutative geometry. In recent pre-printed papers^{33,34}, J. Pearson and J. Bellissard explored

Cantor sets when seen as non-commutative spaces. They have developed a measure theory for distributions having Cantorian support, which notably makes use of Dirichlet series; and, they demonstrate two powerful tools of special interest here: a canonical probability measure on Cantor sets, and the formalization of Brownian motion on the triadic Cantor set, from which they deduce the mean displacement by diffusion in the limit of short times. No doubt that these novel methods will be essential in the quest of a chemical kinetics theory augmented with non-commutativity-dependent properties.

ACKNOWLEDGEMENTS

I wish to thank Dr. V. Cavallès for his astute and helpful pre-reviewing of this paper, Dr. P. Augereau for his straightforward hints about computer materials, and Dr. J. Barbour for his positive and encouraging reply.

APPENDIX A: TREE ESTIMATION WITH MONTE-CARLO METHOD

For each set of pre-determined initial conditions, kinetics constants and chronon value, the map defined by $\varpi_{n+1} = (\varepsilon_n Q_+ Q_- + (1 - \varepsilon_n) Q_- Q_+) \varpi_n$ was iterated up to 30000 times, the value ε_n being the n^{th} item of a sequence of 0's or 1's, which were drawn at random according to a Bernoulli law of parameter $1/2$. Bernoulli process can effectively be generated using the uniform distribution provided by the Bernoulli shift, after it has been stretched and truncated with the ceiling function, i.e. $\varepsilon_n = \lfloor (3^n s_0 \bmod 1) \times 2 \rfloor^{35}$, where s_0 is the initial seed randomly chosen in $[0,1]$. Due to the mass conservation law, the state space of the first-order reversible reaction is bounded to the interval $[0, x_i + y_i]$, so all statistical assessments should be performed within that interval. For each orbit generated, relative frequencies were calculated for a partition of either the whole state space, or of a windowed sub-part of it around analytical equilibrium given by $x_{eq} = (x_i + y_i)(k_- / (k_- + k_+))$ and $y_{eq} = (x_i + y_i)(k_+ / (k_- + k_+))$. Those partitions always consisted in a sub-division into 1024 regions; windowing allowed convenient zooming on a particular sub-set of the tree. Relative frequency in a partition region was calculated counting the number of times ϖ_n has visited this particular region, then dividing the cumulated count by the total number of mapped values, i.e. 30000.

REFERENCES

- ¹ A. Connes, *Noncommutative Geometry*, Academic Press (1994)
- ² B. Escoubès, J. L. Lopes, *Sources et évolution de la physique quantique*, EDP sciences (2005)
- ³ M. Born, and P. Jordan, *Zeitschr. f. Phys.* **34**, 838 (1925)
- ⁴ M. Born, W. Heisenberg, and P. Jordan, *Zeitschr. f. Phys.* **35**, 557 (1926)
- ⁵ J. Geiser, *J. Comp. App. Math.* **217**, 227 (2008)
- ⁶ I. Faragó, and Á. Havasi, *The Mathematical Background of Operator Splitting and the Effect of Non-commutativity*, 3rd International Conference LSSC 2001
- ⁷ L. A. N. Amaral, and J. M. Ottino, *Chem. Eng. Sci.* **59**, 1653 (2004)
- ⁸ J. Elf and M. Ehrenberg, *Genome Res.* **13**, 2475 (2003)
- ⁹ J. Paulsson, and M. Ehrenberg, *Phys. Rev. Lett.* **84**, 5447 (2000)
- ¹⁰ P. B. Warren, S. Tanasa-Nicola, and P. R. ten Wolde, *J. Chem. Phys.* **125**, 144904 (2006)
- ¹¹ V. Privman, M. A. Arugula, Jan Halánek, M. Pita, and E. Katz, *J. Phys. Chem. B* **113**, 5301 (2009)
- ¹² E. M. Ozbudak, M. Thattai, I. Kurtser, A. D. Grossman, and A. van Oudenaarden, *Nature Genetics* **31**, 69 (2002)
- ¹³ P. Caldirola, *Il Nuovo Cim.* **45**, 549 (1978)
- ¹⁴ P. Caldirola, *Lett. Nuovo Cim.* **27**, 225 (1980)
- ¹⁵ H. Konno, and P. S. Lomdahl, *J. Phys. Soc. Jap.* **64**, 1936 (1995)
- ¹⁶ P. Gaspard, *Chaos, scattering and statistical mechanics*, Cambridge University Press (2005)
- ¹⁷ B. Bollobas, *Modern Graph Theory*, Springer-Verlag 1998
- ¹⁸ Another method, which is the most exhaustive one, could have been to calculate all vertices of the tree up to some pre-determined time. However, as state duplication occurs concomitantly along with time, the data generated becomes rapidly overwhelming, since equalling to $2^{n+1} - 1$ vertices per dimension for any n long simulation, proving rapidly limited with standard computation material.
- ¹⁹ T. Gilbert, J.R. Dorfman, and P. Gaspard, *Phys. Rev. Lett.* **85**, 1606 (2000)
- ²⁰ G. Cantor, *Math. Ann.* **21**, 545 (1883)
- ²¹ M. Wilkinson, *Proc. R. Soc. Lond. A* **391**, 1801 (1984)
- ²² D. Canet, *Nuclear magnetic resonance: concepts and methods*, Wiley (1996)

- ²³ G. C. K. Roberts, *NMR of macromolecules: a practical approach*, Oxford university press (1993)
- ²⁴ B. C. Dian, G. G. Brown, K. O. Douglass, F. S. Rees, J. E. Johns, P. Nair, R. D. Suenram, and B. H. Pate, Proc. Natl. Acad. Sci. U.S.A. **105**, 12696 (2008)
- ²⁵ R. W. Schoenlein, L. A. Peteanu, R. A. Mathies, and C. V. Shank, Science **254**, 412 (1991)
- ²⁶ H. Eyring, J. Chem. Phys. **3**, 107 (1935)
- ²⁷ J. D. Roberts, *An Introduction to the Analysis of Spin-Spin Splitting in High Resolution NMR Spectra*, W. A. Benjamin Inc., New York (1961)
- ²⁸ T. Baer, and A. R. Potts, J. Phys. Chem. **104**, 9397 (2000)
- ²⁹ D. B. Borchardt, and S. H. Bauer, J. Chem. Phys. **85**, 4980 (1986)
- ³⁰ P. Tompa, FEBS Lett. **579**, 3346 (2005)
- ³¹ H. J. Dyson, and P. E. Wright, Nat. Rev. Mol. Cell. Bio. **6**, 197 (2005)
- ³² H. J. Dyson, and P. E. Wright, Nat. Struc. Bio. NMR Supp., 499 (1998)
- ³³ J. C. Pearson, *The Noncommutative Geometry of Ultrametric Cantor Sets*, approved thesis dissertation, Georgia Institute of Technology (2008)
- ³⁴ J. Pearson, and J. Bellissard, arXiv:math\0802.1336 v2 (2008)
- ³⁵ J. C. Sprott, *Chaos and time-series analysis*, Oxford University Press (2003)

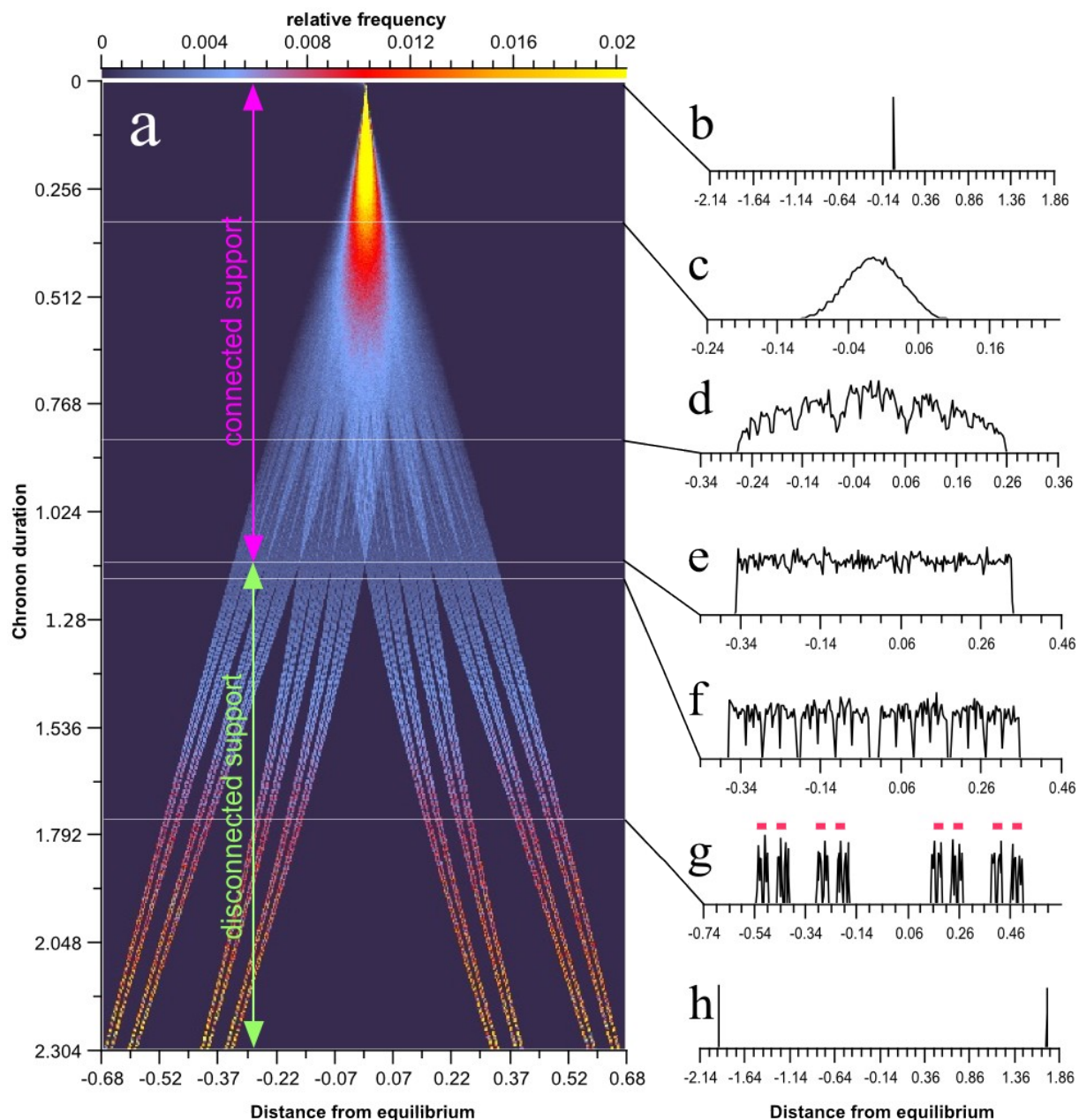


FIG. 1. Non-commutativity-dependent coalescence as a function of chronon duration. Left: (a) Non-equilibrium statistics in a windowed state space defined by the boundary values ± 0.68 , with initial conditions $x_i = 4$ and $y_i = 0$. Each of these white lines labelled from b to h stands for a key-distribution chosen over the continuum of control parameter θ . Right: The so-called key-distributions, where ordinate is the statistical relative frequency. Qualitative characterization of key-distributions: (b) Dirac, (c) Bell-shaped, (d) Takagi function, (e) Uniform, (f) Transition from connected to disconnected support, (g) Cantorian distribution + C_3 indicated with red segments, (h) Bimodal in the limit $\theta \rightarrow +\infty$ (here at $\theta = 10.3989$). Both chemical entities x and y have similar statistics, with respect to the symmetry provided by the mass conservation law $x_n = (x_i + y_i) - y_n$.

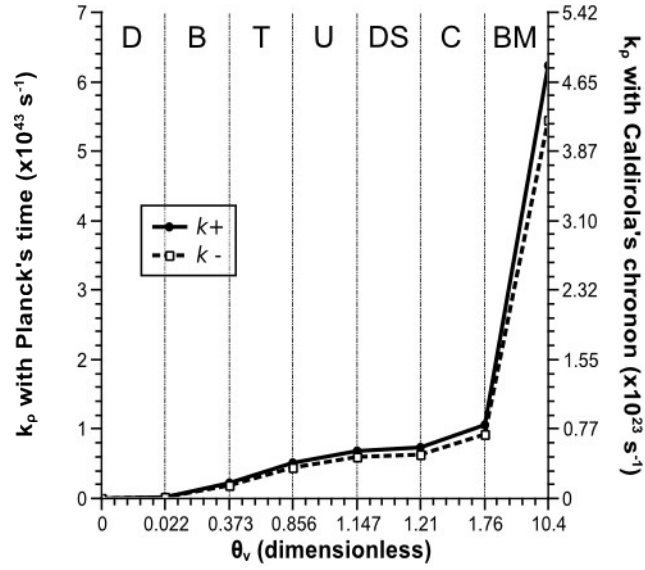


FIG. 2. Real system kinetics constants determination as a function of numerical chronon duration. Function $\varphi(\theta_v) = (k_v / \theta_\rho) \times \theta_v$ was computed with key-values placed at regular intervals, so as to obtain the seven key-phases corresponding to the seven key-distributions on a regular scale. Letters mean D: Dirac, B: Bell-shaped, T: Takagi class function, U: Uniform, DS: From connected to disconnected support phase, C: Cantorian, BM: Bimodal. Constants were chosen such that $k_v = k_+$ or k_- , and $\theta_\rho = 5.37 \times 10^{-44}$ s (left y axis), or $\theta_\rho = 6.97 \times 10^{-24}$ s (right y axis).